Table III. Atomic Parameters for 3

| atom | x/a | y/b | z/c | U(eq)[a] |
|---|---|---|---|---|
| CL1 | 0.2092 (1) | 1/4 | 0.1071 (1) | 0.0617 (4) |
| O1 | 0.3397 (3) | 0.4905 (3) | 0.0964 (4) | 0.055 (1) |
| B1 | 0.2841 (7) | 0.3921 (5) | 0.2319 (7) | 0.048 (2) |
| C1 | 0.7719 (5) | 0.2775 (4) | 0.3703 (5) | 0.046 (2) |
| C2 | 0.6181 (5) | 0.3366 (4) | 0.2527 (5) | 0.044 (1) |
| C3 | 0.4595 (5) | 0.3745 (4) | 0.3549 (5) | 0.042 (1) |
| C4 | 0.4474 (5) | 0.2967 (4) | 0.5151 (5) | 0.044 (1) |
| C5 | 0.6271 (4) | 0.2373 (5) | 0.5789 (5) | 0.045 (1) |
| C6 | 0.7909 (5) | 0.3238 (5) | 0.5558 (5) | 0.047 (2) |
| C7 | 0.6878 (5) | 0.1583 (4) | 0.4366 (6) | 0.053 (2) |
| C8 | 0.9629 (6) | 0.2679 (6) | 0.6504 (6) | 0.071 (2) |
| C9 | 0.7870 (6) | 0.4583 (5) | 0.6004 (7) | 0.060 (2) |
| C10 | 0.6629 (6) | 0.4442 (5) | 0.1443 (6) | 0.057 (2) |
| C11 | 0.5047 (7) | 0.4712 (5) | 0.0126 (7) | 0.062 (2) |
| C12 | 0.1944 (7) | 0.5376 (6) | -0.0212 (8) | 0.078 (2) |
| H1 | 0.160 (6) | 0.422 (5) | 0.280 (6) | 0.067 (4) |

[a] The equivalent isotropic $U$ is defined as one-third of the trace of the orthogonalized $U_{ij}$ tensor.

check reflections showed, in addition to the random statistical variations expected for such measurements, a net 9% decline over the course of the data collection. The data were corrected for this decline by using a linear decay curve. Standard corrections for Lorentz and polarization factors were also applied.

The position of the chlorine atom was determined from a Patterson map. This was input to the program DIRDIF,[30] which gave positions for the other atoms. Tentative assignments of the atom types were based upon the method of synthesis, the NMR data, and the oxidative conversion of **3** to **6**. The assignments were confirmed by examination of isotropic thermal parameters at various stages of refinement and by the final difference electron density map. Least-squares refinement using data set I, with all atoms isotropic, converged with $R_1 = 0.087$ and $R_2 = 0.115$. Further refinement was carried out by using data set II after averaging equivalent reflections; however, Friedel pairs were not averaged. At convergence ($R_1 = 0.104$, $R_2 = 0.137$) with all atoms isotropic, the positions of all hydrogen atoms were clearly visible in the calculated difference electron density map. The hydrogen atoms were then included in the model in idealized $sp^3$ geometries [$d$(C-H) = 1.08 Å] with methyl groups treated as rigid entities. They were refined by using two common isotropic temperature factors, one for the methyl hydrogens and one for the borane hydrogen and other non-methyl hydrogens. This refinement converged with $R_1 = 0.037$ and $R_2 = 0.046$. Because these geometric constraints might be inappropriate for the borane hydrogen, this atom was freed of all constraints in the final model.[31] The results of least-squares calculations on the final model are given in the tables. A final difference electron density map was featureless.

The absolute configuration of **3** (vide supra) was confirmed by using the method of Hamilton.[32] The real and imaginary anomalous dispersion terms were included for the non-hydrogen atoms,[33] and $R_2$ values were calculated for both enantiomers. The ratio of the resulting $R_2$ values (0.0476, 0.0459) is 1.0370, significantly greater than the $R_{1,1000,0.005}$ value of 1.0039. Thus, at the 99.5% confidence level, the absolute configuration shown for **3** is correct.

**Acknowledgment.** We are grateful for financial support provided by the National Institutes of Health, the donors of the Petroleum Research Fund, administered by the American Chemical Society, and Merck, Sharp & Dohme Research Laboratories. We also thank Martin Ashley for assistance in obtaining NMR spectra and Dr. Kurt L. Loening for advice on nomenclature. Dr. Clinton F. Lane of Aldrich Boranes, Inc., graciously provided the procedure for vacuum transfer of $BH_3{\cdot}SMe_2$.

**Registry No. 3** (coordinate structure), 98689-90-8; **3** (borane structure), 98703-99-2; **4**, 35836-73-8; **5**, 81991-72-2; **6**, 98689-91-9; **7**, 98703-98-1; $BH_3{\cdot}SMe_2$, 13292-87-0; $BH_2Cl{\cdot}SMe_2$, 63348-81-2; $BHCl_2{\cdot}SMe_2$, 63462-42-0; (+)-dehydroabietyl isocyanate, 97363-89-8.

**Supplementary Material Available:** Tables of anisotropic thermal parameters, hydrogen atom parameters, and observed and calculated structure factor amplitudes (8 pages). Ordering information is given on any current masthead page.

(30) Beurskens, P. T.; Bosman, W. P.; Doesburg, H. M.; Gould, R. O.; van den Hark, Th. E. M.; Prick, P. A.; Noordik, J. H.; Buerskens, G.; Parthasarthi, V.; BruinsSlot, H. J.; Haltiwanger, R. C. "DIRDIF, Technical Report"; Crystallography Laboratory: Toernooiveld, 6525 ED Nijmegen, The Netherlands, 1983/1.

(31) This treatment of the hydrogen atoms minimizes the number of variables in the refinement and is expected to afford the most accurate interatomic distances involving hydrogen nuclei. We also undertook least-squares refinement of a model with no constraints on any hydrogen atoms. This refinement resulted in no statistically significant shifts (i.e., changes greater than $3\sigma$) in the postional parameters for the non-hydrogen atoms. The C(2)-C(3) bond distance decreased by 0.020 Å and the C(8)-C(6)-C(1) angle increased by 1.2°.

(32) Hamilton, W. C. *Acta Crystallogr.* **1965**, *18*, 502-510.

(33) "International Tables for X-ray Crystallography"; Kynoch Press: Birmingham, England, 1974; Vol. 4.

# *Communications to the Editor*

## Photoelectron Spectrum of [1.1.1]Propellane: Evidence for a Nonbonding MO?

Ev. Honegger, Hanspeter Huber, and Edgar Heilbronner*

*Physikalische-Chemisches Institut, Universität Basel 4056 Basel, Switzerland*

William P. Dailey and Kenneth B. Wiberg*

*Department of Chemistry, Yale University New Haven, Connecticut 06511*

*Received April 4, 1985*

The sequence and overall contours of the bands in the He(I$\alpha$) PE spectrum of [1.1.1]propellane (**1**) (=tricyclo[1.1.1.$0^{1,3}$]pentane)[1,2] (Figure 1) correspond exactly to the expectation based on available molecular orbital calculations,[3] assuming the validity of Koopmans' theorem. For example, the results of ab initio

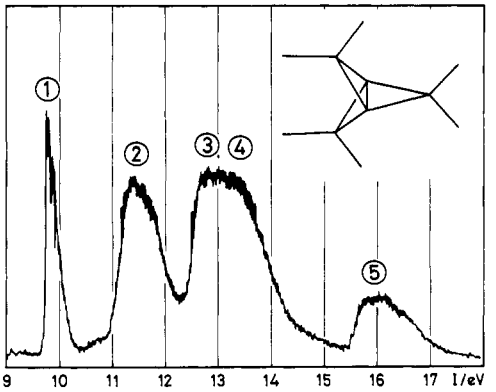


**Figure 1.** He(I$\alpha$) PE spectrum of [1.1.1]propellane (**1**). Sample temperature -10 to -15 °C; temperature 20 °C.

(1) Wiberg, K. B.; Walker, F. H. *J. Am. Chem. Soc.* **1982**, *104*, 5239. Wiberg, K. B. *Acc. Chem. Res.* **1984**, *17*, 379.

0002-7863/85/1507-7172$01.50/0 

**Table I.** Ionization Energies $I_j^m$ and Orbital Energies $\epsilon_j$ of [1.1.1]Propellane

| band | $I_j^m$/eV[a] | orbital[b] | $-\epsilon_j$/eV 6.31G[c] | $-\epsilon_j$/eV FOGO[d] |
|---|---|---|---|---|
| 1 | 9.74 | $3a_1'$ | 9.81 | 9.48 |
| 2 | $11.3_5$ | $1e''$ | 12.01 | 11.75 |
| 3 | $12.6_0$ | $3e'$ | 14.15 | 13.60 |
| 4 | $(13.4_5)$ | $1a_2'$ | 14.72 | 14.53 |
| 5 | 15.7 (16.1) | $2e'$ | 17.83 | 17.51 |

[a] $I_j^m$ = position of band maximum; values in parentheses refer to shoulders. [b] The numbering of the symmetry labels within each irreducible representation refers to the valence-shell orbitals only, i.e., those of carbon 2s and 2p and hydrogen 1s parentage. [c] Taken from ref 3, 10. These values yield the regression, $(I/\text{eV}) = 2.406 + 0.7415(-\epsilon/\text{eV})$; standard errors $s(I) = 0.196$ eV; $s(\text{slope}) = 0.0326$; correlation coefficient $r = 0.9971$. [d] Unpublished; concerning the FOGO procedure, cf. ref 5. These values yield the regression $(I/\text{eV}) = 2.637 + 0.7431(-\epsilon/\text{eV})$; standard errors $s(I) = 0.095$ eV; $s(\text{slope}) = 0.0157$; correlation coefficient $r = 0.9993$.

treatments using an extended, polarized 6-31G* basis[4] or the FOGO procedure[5] (which corresponds to a treatment of DZ+P quality) are given in Table I, together with the corresponding linear regressions. By use of a previously defined test function,[6] which takes care of contributions due to the ordering of the data, it can be shown that both regressions are highly significant. Because **1** is a small molecule of very high symmetry ($D_{3h}$), the orbital sequence is almost entirely symmetry conditioned and there is hardly any doubt that the assignment presented in Table I is the correct one. In particular the typical Jahn–Teller envelopes of bands 2, 3, and 5 point to correspondingly degenerate, and thus Jahn–Teller unstable, states of the radical cation $\mathbf{1}^+$ (i.e., $\tilde{B} = {}^2E''$; $\tilde{C} = {}^2E'$, $\tilde{E} = {}^2E'$), whereas the sharpness of band 1 clearly indicates that the electronic ground state of $\mathbf{1}^+$ is definitely not degenerate, $\tilde{A} = {}^2A_1'$.

In Figure 2 we compare the PE band positions observed for the series of hydrocarbons: cyclopropane (**3**);[7,8] bicyclo[1.1.0]-butane (**2**);[9] [1.1.1]propellane (**1**). Note that $I_1^m$ is not a monotonic function of the number of three-membered rings! It is gratifying that the observed trend is predicted by the 6-31G* calculations:[3,10] **3**, $\epsilon_1 = -11.35$ eV; **2**, $\epsilon_1 = -9.71$ eV; **1**, $\epsilon_1 = -9.81$ eV.

The most remarkable features of the PE spectrum of **1** are (1) that the 0,0 vibrational component of the first band (1) is the most intense one, which means that the adiabatic ionization energy $I_1^a$ is very close to the vertical one $I_1^a \sim I_1^v$ ($\sim I_1^m$) and (2) that the half-width at half-height (hwhh) of band 1 is extremely narrow, namely, only 0.25 eV. For comparison, one observes for the first band in the PE spectrum of the closely related bicyclo[1.1.0]butane (**2**) a hwhh = 0.73 eV[9] and for the bands in the PE spectra of small, saturated hydrocarbons typical values of hwhh > ~0.7 eV.[8]

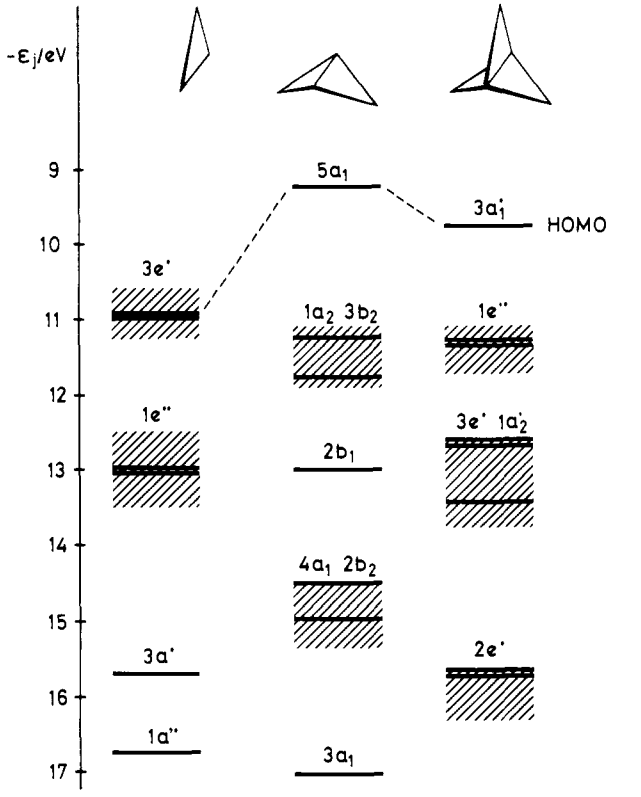


**Figure 2.** Orbital correlation diagram for cyclopropane (**3**), bicyclo-[1.1.0]butane (**2**), and [1.1.1]propellane (**1**). The orbital energy values given correspond to the observed positions of the bands in the PE spectra, i.e., $\epsilon_j = -I_j^m$. The shaded areas indicate overlapping bands or bands broadened by the Jahn–Teller effect.

This is a clear indication that ionization of **1** to yield ground-state $\mathbf{1}^+$, i.e., electron ejection from the HOMO $3a_1'$ of **1**, leads to only minute changes in geometry of the molecular frame. This experimental observation is fully supported by the results of FOGO calculations for **1** and $\mathbf{1}^+$ (complete energy minimization under $D_{3h}$ symmetry restriction) which yield a *shortening* of the central CC bond on ionization by $\Delta R_{1,3} = -3.5$ pm, a slight lengthening of the six others by $\Delta R_{1,2} = +0.9$ pm, practically zero change of the CH bond lengths $\Delta R_{CH} = -0.1$ pm, and a slight widening of the HCH angle, $\Delta\theta = +1.6°$. It could be argued that the lack of structural change accompanying the transition $\mathbf{1} \rightarrow \mathbf{1}^+$ is a consequence of the predicted nonbonding or slightly antibonding[3] character of the HOMO $3a_1'$ of **1** (cf. ref 1, 11, 12). However, the rather tight cage structure of **1**, which leaves little leeway for geometric distortions, could also be the determining factor.

To conclude, we wish to draw attention to an unresolved problem connected with the PE spectrum of **1**. From an expanded recording of the fine structure of band 1 (using Ne(I) radiation), one finds that the separation of the first two vibrational components is only $0.04_5$ eV ($\sim 360 \pm 20$ cm$^{-1}$), which is *much smaller* than $\nu_{12} = 529$ cm$^{-1}$, the wavenumber of the lowest frequency vibration observed for **1**.[12] However, this mode is not totally symmetric but belongs to E'. The mode of type $A_1'$ with lowest frequency has $\nu_4 = 908$ cm$^{-1}$. According to preliminary FOGO calculations, one would expect that the low-frequency $A_1'$ mode should be found at *higher* wavenumbers in the radical cation $\mathbf{1}^+$ than in the parent hydrocarbon **1**. Changing the length of the central bond by $\pm 0.05a_0 = 2.65$ pm and minimizing the total energy with respect to the remaining bond distances and angles under imposed $D_{3h}$ symmetry yields an overall force constant for

(2) The molecule **1** tends to rearrange to 3-methylenecyclobutene.[1] The prominent, first $\pi^{-1}$ band in its PE spectrum is found at $I_1^m = 8.88$ eV (unpublished results, Basel). Within the limits of the signal to noise ratio, this band is absent from the PE spectrum presented in Figure 1.

(3) Newton, M. D.; Schulman, J. M. *J. Am. Chem. Soc.* **1972**, *94*, 773. Stohrer, W.-D.; Hoffmann, R. *Ibid.* **1972**, *94*, 779. Wiberg, K. B. *Ibid.* **1983**, *105*, 1227. Wiberg, K. B.; Wendoloski, J. J. *Ibid.* **1982**, *104*, 5679. Jackson, J. E.; Allen, L. C. *Ibid.* **1984**, *106*, 591 and references given therein. See also: Epiotis, N. D. "Unified Valence Bond Theory and Electronic Structure. Applications"; Springer Verlag: New York, Berlin, 1983.

(4) Harihan, P. C.; Pople, J. A. *Theor. Chim. Acta* **1973**, *28*, 213.

(5) Huber, H. *Theor. Chim. Acta* **1980**, *55*, 117. The FOGO (floating orbital geometry optimization) procedure uses floating outer-shell basis functions which are shifted to an optimal polarized position and reproduce the effect of polarization functions.

(6) Heilbronner, E.; Schmelzer, A.; *Nouv. J. Chim.* **1980**, *4*, 23.

(7) Basch, H.; Robin, M. B.; Kuebler, N. A.; Baker, C.; Turner, D. W. *J. Chem. Phys.* **1969**, *51*, 52.

(8) Kimura, K.; Katsumata, S.; Achiba, Y.; Amazaki, T.; Iwata, S. "Handbook of He I Photoelectron Spectra of Fundamental Organic Molecules"; Japan Scientific Societies Press: Tokyo, 1981.

(9) Bombach, R.; Dannacher, J.; Stadelmann, J.-P.; Neier, R. *Helv. Chim. Acta* **1983**, *66*, 701.

(10) Unpublished data, Yale University.

(11) Dunitz, J. D. "X-Ray Analysis and the Structure of Organic Molecules"; Cornell University Press: Ithaca, NY, 1979; p 391 ff. Chakrabarti, P.; Seiler, P.; Dunitz, J. D.; Schlüter, A.-D.; Szeimies, G. *J. Am. Chem. Soc.* **1981**, *103*, 7378.

(12) Wiberg, K. B.; Dailey, W. P.; Walker, F. H.; Waddell, S. T.; Crocker, L. S.; Newton, M. *J. Am. Chem. Soc.*, in press.

such a deformation of $k = 483$ N m$^{-1}$ for **1** and $K = 640$ N m$^{-1}$ for $\mathbf{1}^+$. This result contradicts what is observed (and by far!) if one assumes that only totally symmetric vibrational modes are stimulated by electron ejection from $3a_1'$. One, as yet unexplored, explanation for the observed, close spacing of the vibrational fine structure of band 1 could be looked for in the vibronic mixing of the $^2A_1'$ ground state of $\mathbf{1}^+$ with the first excited $^2E''$ state, which are only ~1.0 eV apart (adiabatically).

**Acknowledgment.** This investigation was supported by the Schweizerischer Nationalfonds zur Förderung der Wissenschaftlichen Forschung and NSF Grant CHE-85-01023 (Yale).

**Registry No. 1**, 35634-10-7.

## Rotational Spectra and Structures of Small Clusters: $Ar_3$–HF and $Ar_3$–DF

H. S. Gutowsky,* T. D. Klots, Carl Chuang, John D. Keen, C. A. Schmuttenmaer, and Tryggvi Emilsson

*Noyes Chemical Laboratory, University of Illinois Urbana, Illinois 61801*

*Received April 1, 1985*

Previous studies of microwave rotational spectra for van der Waals and hydrogen bonded complexes have been limited to binary species like Ar–HF[1,2] and $(HF)_2$.[3-5] Herein we demonstrate the feasibility of extending such studies to small molecular clusters. In particular, we report the characterization of $Ar_3$–HF and $Ar_3$–DF, in which the H/DF lies along the threefold ($c$) axis of the $Ar_3$ group, with the H/D end closest to $Ar_3$. The symmetric top transitions observed for $J = 1 \rightarrow 2$ through $J = 6 \rightarrow 7$ are fitted by rotational constants $B_0$, $D_J$, and $D_{JK}$ of 1188.212 MHz, 6.85 kHz, and −5.76 kHz for $Ar_3$–HF and of 1180.379 MHz, 6.57 kHz, and −5.15 kHz for $Ar_3$–DF. The composition of the clusters is established by hyperfine structure of the transitions, by the absence of $K$ states other than 0, ±3, and ±6, and by the values found for $B_0$.

The spectra were observed with the Flygare Mark II spectrometer.[6] It combines the principles of pulsed Fourier transform spectroscopy, a Fabry-Perot cavity, and synchronization of the microwave pulse with a pulsed beam of a gas mixture from a supersonic nozzle which cools the gas mixture and helps generate the molecular complexes.[7] Detection of the cluster was made possible by modifications in the spectrometer which increased S/N about 10-fold by better utilization of its inherent sensitivity.[8] The main improvements were the use of several microwave pulses after each gas pulse, a 10-fold increase in the repetition rate of the gas pulse, and mounting the gas nozzle to enable ready adjustment of its distance from the axis of the Fabry-Perot mirrors. Also, a microwave coupling system was developed to extend the cavity's operating range to C band (4–8 GHz).[8]

Argon was used as the carrier gas with 0.5–1.0% of HF and/or DF added. At the nozzle the gas mixture was at ambient temperature and 1 atm. The nozzle diameter was 0.94 mm. Under these conditions Ar–HF and $(HF)_2$ are readily observed,[1-4] and small clusters of $Ar_n$[9,10] and $(HF)_n$[3] are generated at concentrations decreasing with $n$. Also, mixed species $Ar_n$–$(HF)_m$ are formed, with Ar–$(HF)_2$ and $Ar_2$–HF expected to predominate.[10] Indeed, we have observed a large number of transitions attributed tentatively to $Ar_2$–HF (T shaped), Ar–$(HF)_2$, and a noncyclic $(HF)_3$. The most fully characterized species, however, is a symmetric top, which has the more readily identifiable transitions listed in Table I for HF. They were fitted by the usual Hamiltonian including centrifugal distortion.[11] An equivalent set of transitions was observed at somewhat lower frequencies with DF.

Although the $J = 0 \rightarrow 1$ transitions are below the present frequency range, the weaker, less extensive hyperfine structure was observed for the $K = 0$, $J = 1 \rightarrow 2$ transitions[2] (Table II). It establishes the presence of an H/DF molecule at the figure axis of the symmetric top, without perturbations from other $I \neq 0$ nuclei. The hyperfine structure was fitted as done earlier[2] for the Ar–HF and Ar–DF dimers. The adjustable parameters are the line center and the "average" torsional angle $\alpha$ between the H/DF axis and the $c$-inertial axis, which reduces the hyperfine interactions by the factor $\langle 3\cos^2\alpha - 1\rangle/2$. The values found for $\alpha$ in the HF and DF species are 41.0 (2)° and 35.6 (4)°, compared with 41.1° and 32.7° reported for the dimers.[2] The similarity indicates the equilibrium configuration has the H/DF axis along the $c$ axis.

Transitions were observed for only two nonzero $K$ states, assigned in Table I as $K = \pm 3$ and ±6.[12] An alternate assignment is as $K = \pm 1$ and ±2, with the higher states too weak for detection. This is precluded, however, by the observed partially resolved lines listed as $K = \pm 3$ for $J = 3 \rightarrow 4$ and $J = 4 \rightarrow 5$. They extend over ~50 and 20 kHz, respectively, in accord with calculations

**Table I.** Observed and Calculated Frequencies of the Rotational Transitions for $Ar_3$–HF[a]

| $J,K \rightarrow J',K'$ | obsd, MHz | calcd, MHz | difference, kHz |
|---|---|---|---|
| 1,0 → 2,0 | 4752.628 | 4752.630 | −2 |
| 2,0 → 3,0 | 7128.533 | 7128.535 | −2 |
| 3,0 → 4,0 | 9503.944 | 9503.946 | −2 |
| 3,±3 → 4,±3 | 4.37[b] | 4.362 | |
| 4,0 → 5,0 | 11878.699 | 11878.700 | −1 |
| 4,±3 → 5,±3 | 9.21[b] | 9.219 | |
| 5,0 → 6,0 | 14252.636 | 14252.632 | 4 |
| 5,±3 → 6,±3 | 3.257 | 3.254 | 3 |
| 6,0 → 7,0 | 16625.579 | 16625.578 | 1 |
| 6,±3 → 7,±3 | 6.300 | 6.303 | −3 |
| 6,±6 → 7,±6 | 8.479 | 8.479 | 0 |

[a] Transition frequencies for states with $K \neq 0$ are emphasized by omitting the first 3 or 4 digits, which are the same as for the transition just above. [b] Approximate center of partially resolved hyperfine structure; not used in determination of rotational constants.

**Table II.** Observed and Calculated Frequencies of the Hyperfine Components in the $K = 0$, $J = 1 \rightarrow 2$ Transitions

| components | | | obsd, | calcd, | difference, |
|---|---|---|---|---|---|
| $J,F_1,F$ | → | $J',F_1',F'$ | MHz | MHz | kHz |
| Transition at 4752.628 MHz for HF Species | | | | | |
| $1,{}^3/_2,2$ | | $2,{}^3/_2,2$ | 2.597 | 2.597 | 0 |
| $1,{}^1/_2,0$ | | $2,{}^3/_2,1$ | 2.603 | 2.602 | 1 |
| $1,{}^1/_2,1$ | | $2,{}^3/_2,2$ | 2.628 | 2.628 | 0 |
| $1,{}^3/_2,1$ | | $2,{}^5/_2,2$ | | 2.628 | 0 |
| $1,{}^3/_2,2$ | | $2,{}^5/_2,3$ | | 2.630 | −2 |
| $1,{}^1/_2,1$ | | $2,{}^3/_2,1$ | 2.679 | 2.678 | 1 |
| Transition at 4721.304 MHz for DF Species | | | | | |
| $1,1,{}^3/_2$ | | $2,1,{}^3/_2$ | 1.215[a] | 1.216 | −1 |
| $1,1,{}^1/_2$ | | $2,2,{}^3/_2$ | 1.300 | 1.298 | 2 |
| $1,2,{}^3/_2$ | | $2,3,{}^5/_2$ | | 1.299 | 1 |
| $1,2,{}^5/_2$ | | $2,3,{}^7/_2$ | | 1.301 | −1 |
| $1,1,{}^3/_2$ | | $2,2,{}^5/_2$ | 1.307 | 1.306 | 1 |
| $1,0,{}^1/_2$ | | $2,1,{}^3/_2$ | 1.341 | 1.343 | −2 |

[a] The first 3 digits are omitted.

(1) Dixon, T. A.; Joyner, C. H.; Baiocchi, F. A.; Klemperer, W. *J. Chem. Phys.* **1981**, *74*, 6539.
(2) Keenan, M. R.; Buxton, L. W.; Campbell, E. J.; Legon, A. C.; Flygare, W. H. *J. Chem. Phys.* **1981**, *74*, 2133.
(3) Dyke, T. R., Howard, B. J., Klemperer, W. *J. Chem. Phys.* **1972**, *56*, 2442. Howard, B. J.; Dyke, T. R.; Klemperer, W. *J. Chem. Phys.* **1984**, *81*, 5417.
(4) Gutowsky, H. S.; Chuang, C.; Keen, J. D.; Klots, T. D.; Emilsson, T. *J. Chem. Phys.* **1985**, *83*, 2070.
(5) See, for example, Leopold, K. R. (Ph.D. Thesis, Harvard University, 1983), who describes an inconclusive search for $Ar_2$-OCS.
(6) Campbell, E. J.; Read, W. G.; Shea, J. A. *Chem. Phys. Lett.* **1983**, *94*, 69.
(7) Balle, T. J.; Campbell, E. J.; Keenan, M. R.; Flygare, W. H. *J. Chem. Phys.* **1980**, *72*, 922.
(8) Emilsson, T.; Gutowsky, H. S., unpublished results.
(9) Golomb, D.; Good, R. E.; Brown, R. F. *J. Chem. Phys.* **1970**, *52*, 1545.
(10) Bowen, K. H., Jr. Ph.D. Thesis, 1977, Harvard University.
(11) Townes, C. H.; Schawlow, A. L. "Microwave Spectroscopy"; McGraw-Hill: New York, 1955; pp 48–82.
(12) We thank a referee for helping us mind our $J$'s and $K$'s.

0002-7863/85/1507-7174$01.50/0 